IJMCM
Winter 2019, Vol 8, No 1
DOI: 10.22088/IJMCM.BUMS.8.1.24

Original Article

# Composite Nanoscaffolds Modified with Bio-ceramic Nanoparticles (Zn2SiO4) Prompted Osteogenic Differentiation of Human Induced Pluripotent Stem Cells

Raheleh Halabian[1], Kaykhosro Moridi[2], Mohsen Korani[3], Marzieh Ghollasi[4*]

*1. Applied Microbiology Research Center, Systems Biology and Poisonings Institute, Baqiyatallah University of Medical Sciences, Tehran, Iran.*

*2. Department of Medical Nanotechnology, Faculty of Advanced Sciences & Technology, Pharmaceutical Sciences Branch, Islamic Azad University (IAUPS), Tehran, Iran.*

*3. Chemical Injuries Research Center, Systems Biology and Poisonings Institute, Baqiyatallah University of Medical Sciences, Tehran, Iran.*

*4. Department of Cell and Molecular Biology, Faculty of Biological Science, Kharazmi University, Tehran, Iran.*

*Submmited 12 March 2019; Accepted 15 June 2019; Published 26 June 2019*

Nanofiber scaffolds and bio-ceramic nanoparticles have been widely used in bone tissue engineering. The use of human- induced pluripotent stem cells (hiPSCs) on this scaffold can be considered as a new approach in the differentiation of bone tissue. In the present study, a polyaniline-gelatin-polycaprolactone (PANi-GEL-PCL) composite nanoscaffold was made by electrospinning and modified superficially by plasma method. The synthesized nanoscaffold was then coated with willemite's bio-ceramic nanoparticles ($Zn_2SiO_4$). The nanoscaffold's properties were studied by scanning electron microscopy (SEM). Also, nanoparticles characterization was carried out with SEM and dynamic light scattering. The growth and proliferation rate of cells on the synthesized nanoscaffold was examined by MTT assay. Subsequently, hiPSCs were cultured on murine fibroblast cells, incubated in embryoid bodies for 3 days, and placed on the nanoscaffolds. The differentiation potential of hiPSCs was investigated by the examination of common bone markers (e.g. alkaline phosphatase, calcium salt precipitation, and alizarin red test) using bone differentiation factors for 14 days. SEM showed the proper structure of electrospinned nanoscaffolds and coating of nanoparticles on the nanoscaffold surface. The results of MTT assay confirmed the growth and proliferation of cells and the biocompatibility of nanofibers. The results of bone indices also showed that differentiation on the composite nanoscaffold coated with willemite's bio-ceramic nanoparticles dramatically increased in comparison with other groups. Overall, this study demonstrated that PANi-GEL-PCL composite nanoscaffold with willemite's bio-ceramic nanoparticles is a suitable substrate for *in vitro* growth, proliferation, and differentiation of hiPSCs cells into osteoblasts.

**Key words**: Osteoblast differentiation, Human induced pluripotent stem cells, Poly- aniline- gelatin-polycapro-lactone, $Zn_2SiO_4$ bio- ceramic nanoparticle

*Corresponding author: Department of Cell and Molecular Biology, Faculty of Biological Science, Kharazmi University, Tehran, Iran. Tehran, Iran. Email: ghollasi@khu.ac.ir



[ DOI: 10.22088/IJMCM.BUMS.8.1.24 ]

Tissue engineering is in fact an interdisciplinary field that applies the principles of engineering and natural sciences to the development of functional replacement for damaged tissues (1). Three basic factors should be considered to achieve successful tissue restoration: cells, scaffolds, and bio-molecules (e.g. growth factors, genes, etc.). Two strategies are currently integrated as the best tissue engineering methods. In one of these methods, the scaffold complex is synthesized and previously cultured cells are placed in the damaged area. In this method, the cultivated cells are ultimately separated entirely from the target host tissue, which are in fact the main sources for the formation of newborn tissues. Another method is to replace the damaged tissue by a cell-less scaffold immediately after damage. The principle governing this approach is that proper biological molecules are brought to the affected area using scaffolding, thereby; biological molecules are released from the scaffold in a controlled manner (2, 3).

Beyond these strategies, there is an ever-increasing demand for bioactive scaffolds to achieve successful tissue engineering, which is more than merely a physical support for cells; it also provides the release of biomolecules that affect the regeneration of tissue environment. These types of scaffolds are called "bioactive scaffolds".

Various biomolecules can be incorporated into tissue engineering scaffolds to enhance their functional properties for biomedical applications. Frequently used bio-molecules are proteins (e.g. growth factors and cytokines), and the genes encoding growth factors. Growth factors are endogenous proteins that are capable of adhesion to cell surface receptors, and directing cellular activity involved in new tissue regeneration. Therefore, they are also important contributors to tissue regeneration. However, it can be emphasized that successful direct release of growth factors from scaffolds depends on large-scale production of recombinant growth factors, which is very expensive (4). In addition, protein bioactivity should also be taken into account when placed inside the scaffold (3).

Today, healing of bone injuries caused by accidents have become one of the major problems encountered by hospitals and clinics around the world. Congenital defects or bone loss due to various diseases also exacerbate this problem. Despite advances in medical and pharmaceutical technologies, the number of bone defects and diseases have not decreased significantly due to reduced average life expectancy, increasing population growth, environmental pollution, and tensions from the mechanized life (5).

The demand for tissue engineering scaffolds has considerably risen in recent years. Basic properties of tissue engineering scaffolds should be based on the standards of the Otto bond as these bonds have so far been successful and have been associated with no problems (6, 7).

An ideal scaffold is the one that simulates the biological and structural functions of extracellular matrix either physically or chemically. One of the most important characteristics of the extracellular matrix is its nano-scale structure, which improves cellular function and cellular adhesion (8, 9). In fact, nanofiber scaffolds simulate extracellular matrix structure because of their high fiber-to-diameter ratios and very high contact surfaces, which certainly make a very large contribution to cellular adhesion and proliferation. So far, researchers have shown that nanofibrous scaffolds can play an important role in tissue engineering through creation of an appropriate space for adhesion, proliferation, and differentiation of cells (10-12).

Polycaprolactone (PCL) is a hydrophobic semi-crystalline polymer of the molecular formula $(C_6H_{10}O_2)n$, with such features as mechanical flexibility, good biocompatibility, simple and easy process ability, low melting point, and non-toxicity of the product resulting from its degradation. It is





[ DOI: 10.22088/IJMCM.BUMS.8.1.24 ]

also used in medical sciences due to its flexible structure and a low biodegradability rate. The Food and Drug Administration (FDA) has endorsed PCL as a biodegradable polyester. Polyaniline is one of the oldest synthetic conductive polymers with a high electrical conductivity, which has received considerable attention (13).

The successful use of tricalcium phosphate as a bioceramic agent has been reported in the 20$^{th}$ decade. Bioceramic tricalcium phosphate is currently used and is an example of biochemical absorption. Willemite ($Zn_2SiO_4$) is also a zinc-containing absorbable silica bioceramic, the zinc of which is a necessary ingredient for osteogenesis and avoids oxidative radicals generated by hydrogen peroxide and other free radicals (14).

Stem cells are non-differentiated cells and have several specific characteristics that distinguish them from other cells. Firstly, they have self-renewal ability, hence, they can produce a completely similar cell in terms of function and potency. Secondly, they can differentiate into various types of cells (cardiac, neurological, muscular, etc.) in special physiological or laboratory conditions (15).

Induced pluripotent stem cells (iPSCs) have been successfully produced and their great abilities have been proven in recent studies. An iPS cell is actually an induced form of a differentiated cell that has similar pluripotent characteristics to embryonic stem cells (16). Embryonic stem cells have a high potential for use in restorative medicine, but still some key questions need to be answered before these potent cells can be used at the clinical phase. The nuclear transfer solves the problem of rejection by the immune system.

The goal of restorative medicine is to provide new solutions for patients with a range of chronic degenerative diseases often caused by a specific genetic background. Due to progressive cellular degradation and loss of functional tissues, degenerative diseases are largely responsible for chronic disabilities that the patient suffers from throughout lifespan. This ever-increasing need for new therapies imposes a therapeutic pattern to repair corrupted cell structures. The advent of restorative medicine expands treatment options through the creation of new approaches (17).

The present research investigated the role of $Zn_2SiO_4$ in the differentiation of human iPSCs (hiPSCs) into osteoblasts on a surface-modified PANi-GEL-PCL nanocomposite.

## Materials and methods

### Cultivation and proliferation of hiPSCs

The hiPSCs were obtained from the cell bank of Research Center for Stem Cell Technology (Tehran, Iran). The proliferation of these cells, as many of their properties, was similar to that of embryonic stem cells and included different stages. First the gelatinization of Petri dishes or flasks' bottom was performed by 0.1% gelatin prepared from dissolving 1 g of gelatin powder in 100 µl of saline phosphate buffer. The gelatin solution was autoclaved before use. After gelatinization, the Petri dishes were incubated for 24 h. The preparation of the nutritional layer was done following gelatinization, the gelatin solution was collected from the Petri bottom and DMEM-high glucose medium (Invitrogen, USA) containing 10% FBS (Gibco, Germany), was added to prevent drying of the Petri's bottom. Afterward, SNL as nutritional cells (a class of murine fibroblastic cells) were cultured on the gelatin. The cells were centrifuged at 1200 rpm for 5 min and cultured on gelatinized Petri dishes. Inactivation of murine fibroblastic cells was performed once their density reached 65% to 75%. To inactivate the cells, DMEM solution containing 0.4 mg/ml of mitomycin C (PubChem, USA) was first prepared, the supernatant was discarded, SNL cells were washed with PBS (Sigma, USA), and cells were transferred to the medium containing mitomycin (no FBS). Following 3 h of incubation in 2.5% of $CO_2$ and 35 °C, the





[ DOI: 10.22088/IJMCM.BUMS.8.1.24 ]

medium containing mitomycin wass removed and washed twice with PBS. The hiPSCs medium is then poured onto SNL cells. To cultivate hiPSCs, hiPSCs obtained from the cell bank were defrosted by incubating the cryovial tubes containing hiPSCs in a water bath at 35 °C. Prior to complete defrosting of the frozen cells, they were transferred to the prepared 10% DMEM/FBS medium and centrifuged at 700 rpm for 3 min. The cell cultures last about 2 days, after which their colonies were usually visible under a microscope. Passage and freezing of hiPSCs was accomplished when colonies of hiPSCs were so enlarged (a density of 80 to 90%) that they needed passage. An appropriate nutritional layer was prepared followed by their inactivation (as described above), the hiPSCs supernatant was removed, and the cells washed with PBS. The enzyme collagenase IV (STEMCELL Technologies, Vancouver, Canada) (1 mg/ml) was added to the cells and incubated at 35 °C and 5% $CO_2$ for 2-4 min. Once colonies of hiPSCs were suspended, the collagenase IV was inactivated by a serum medium, and the colonies were transferred into a 15 ml falcon tube, and centrifuged at 700 rpm for 3 min. Afterward, the colonies were ready to be transferred on pre-prepared nutritional layers.

To form embryoid body (EB) formation from hiPSCs, first colonies of hiPSCs were isolated from the nutritional cells by collagenase IV, crushed into smaller pieces by pipetting, and then transferred into non-adhesive six-well plates for the formation of spheroidal EBs. The medium used was the same as that used for hiPSCs but without bFGF growth factor. The cells were treated for 3 days at this stage.

**Synthesis of nanofibrous scaffolds**

To synthesize nanofibrous scaffolds, polyethylene was prepared with a molecular weight of 100,000. First, 1.8 g PCL was dissolved in 9 ml formic acid. Then, 0.1 g poly aniline was dissolved in 1 ml formic acid and then added into the PCL solution. After homogenization of the solution, an electrospining device was adjusted with a voltage of 30, a distance from the collector of 17 cm, and a discharge of 0.5. At the same time, 0.8 g gelatin was dissolved in 5 ml acetic acid and electrospinning conditions were set at a voltage of 17, a distance of 15 cm, and a discharge of 0.4. Then, two-nozzle electrospinning was conducted for the collector at 500 rpm. Finally, the two solutions were combined on the collector making up the composite nanoscaffold.

**Surface modifications of scaffolds with plasma treatment**

A model of nano device from Dimmer Electronic Co. (Germany) was employed to carry out plasma surface modification. Plasma was processed by a low frequency generator with a frequency of 40 kHz inside a cylindrical quartz reactor. After the vacuum was applied, oxygen gas (99.99%) was blown into the reaction chamber and the ambient pressure was fixed at 0.4 mbar. Plasma was processed for 2 min, after which the ambient chamber vacuum was broken and the samples were exposed to the air.

**Contact angle measurement**

After chemical modifications, the hydrophilicity of the scaffolds was examined through measurement of water/scaffold contact angle by the adhesive droplet method using a contact angle measuring device (OCA 15 plus, Kruss, Germany) at room temperature. To do this, a drop of water was placed on the surface of the nanoscaffold and the contact angle was read after 10 s.

**Dynamic light scattering of willemite nanoparticles**

The nanoparticles diameter was determined by dynamic light scattering (DLS, ZSP, Malvern Instrument, and Worcestershire, UK) analysis. Zn2SiO4 nanoparticles were prepared in ethanol anhydrous at 0.1 mg/ml concentration. The size distribution and zeta potential analysis of





[ DOI: 10.22088/IJMCM.BUMS.8.1.24 ]

nanoparticles were evaluated by dynamic light scattering instrument equipped with helium-neon laser and scattering angle.

**Cell growth and proliferation (MTT) assay**

In this study, MTT assay was applied to compare the growth and proliferation of stem cells on nanofibrous scaffolds in four groups including wells containing stem cells, nanofibrous loaded with willemite nanoparticles, wells containing scaffolds without willemite nanoparticles, and wells containing willemite nanoparticles alone. The crushed and sterilized scaffolds from the previous stages were placed into a 24-well cell culture vessel with 10,000 cells on each scaffold. The culture medium was incubated at 37 °C and 5% of $CO_2$ for 2 h. Then, 500 µl of culture medium was added to each well. At 1, 4, and 7 days after this primary culture and at a specific time, 50 µl of MTT solution (5 mg/ml in the base medium) was added to each well and the culture vessel was incubated for 3 h.

The absorbance of purple solution obtained was measured at 570 nm. Also, the wells without a scaffold were used as the control in which the cells were cultivated directly on the surface of the flask. Finally, the numbers of cells on the scaffolds and wells were determined according to the prepared calibration curves. Cell growth and proliferation was tested for each scaffold in triple replicates and the results were reported as mean values.

**Sterilization of scaffolds**

First, each scaffold prepared for cellular processes was cut into circles (with a diameter of 0.5 cm) using a punch. To sterilize the excised scaffolds, each side of the scaffolds was immersed in a 70% ethanol solution for 12 h. Finally, to ensure no microbial contamination, the sterilized scaffolds were placed in a culture medium enriched with FBS for 24 h to determine likely microbial contaminations.

**Willemite nanoparticle coating onto the composite nanoscaffolds**

Willemite nanoparticle powder (10 mg) was poured in a 15 ml falcon tube containing 10 ml deionized distilled water, vortexed, and sonicated for 10 min until the nanoparticles were completely immersed in distilled water. Then, aliquots of the solution containing the nanoparticles were added depending on the numbers of samples and wells in the plates, followed by re-sterilization with 70% alcohol for one day of loading nanoparticles on the scaffolds.

**Culture and bone differentiation of hiPSCs on nanofibrous scaffolds**

To evaluate bone differentiation, hiPSCs were placed on circular scaffold plates after 5 days. The hiPSCs were counted before the transfer, and approximately 40,000 cells were placed on circular scaffolding plates, which were ultimately immersed in the medium. After one day, the basal medium was replaced with a basal medium containing bone fragments. The change of differentiation medium continued as thrice a week until the end of $14^{th}$ day to maintain cells and induce bone formation.

**Scanning electron microscopy**

The structure of willemite nanoparticles, PANi-GEL-PCL nanofibers, and the presence of nanoparticles as well as the shape and morphology of the adhered and differentiated cells on the nanofibrous scaffolds were examined by scanning electron microscope (SEM, KYKY-EM3200, Japan). The surfaces of samples examined by SEM must have electrical conductivity, otherwise, electrons radiated to the sample surface will remain therein and will either repel or deflect resulting in an unstable resultant image. To solve the problem of non-conductivity of polymer nanofibers, a thin layer of gold was applied on the surfaces of the samples using sputter coater method to induce surface conductivity.

**Measurement of alkaline phosphatase activity**

To measure alkaline phosphatase enzyme activity, the total protein from the cells placed on the nanoscaffolds, the nanoparticles coated at the





[ DOI: 10.22088/IJMCM.BUMS.8.1.24 ]

plate bottom, and the control wells were extracted using RIPA buffer solution (200 µl). The enzyme activity was then assessed using a commercial kit (ParsAzmoon Co., Iran) containing the enzyme substrate called para nitrophenol. Alkaline phosphatase provided in the kit was also used as a standard. Enzyme activity (IU/l) was normalized to total protein content (mg/dl).

**Alizarin Red staining**

This method was used to stain the calcium deposits formed on the differentiated stem cells on nanoscaffolds, coated nanoparticles at the plate bottom, and control wells. After washing the differentiated cells with PBS, an appropriate amount of Alizarin Red was added onto the cells for 5-10 min, and then rinsed again with PBS followed by light microscopy imaging.

**Measurement of calcic sediment content**

To measure the amount of calcium deposited on differentiated stem cells on the nanoscaffolds, coated nanoparticles at the plate bottom, and control wells, all of the precipitated salts were first extracted with 0.6 N HCl. Then, calcium content was measured using a commercial kit (Pars Azmoon). The standard calcium solution in the kit was also used to produce a standard optical absorption curve based on the concentration.

**Statistical analysis**

All experiments were conducted at least 3 times and data are expressed as the mean ± standard deviation (SD). One–way ANOVA - Post hoc analysis - least significant difference test was used for analysis of variance. The statistical significance level was set to 0.05 (*).

## Results

**Culture and proliferation of SNL cells as the nutritional layer**

SNL cells are of fibroblastic origin, which are indeed the fibroblast class in the mouse embryo. The cells obtained from the cell bank were cultured and their morphology is shown in Figure 1a. After reaching a density of 11-21%, the cells were incubated in mitomycin C for 3 h. It should be noted that their inactivation is through interference in the cell division cycle. The morphology of the cells varies slightly after inactivation, as shown in Figure 1b.

These cells grow as spherical colonies on the nutritional layer. After the hiPSCs were defrosted, the cells were transferred onto Petri dishes (6 cm) coated with gelatin, cultured with the inactivated SNL nutritional layer, and incubated at 35 °C and 5% of $CO_2$ to reach a density of 80-90%. After a week, colonies of hiPSCs were observed with a completely normal morphology (Fig. 1).

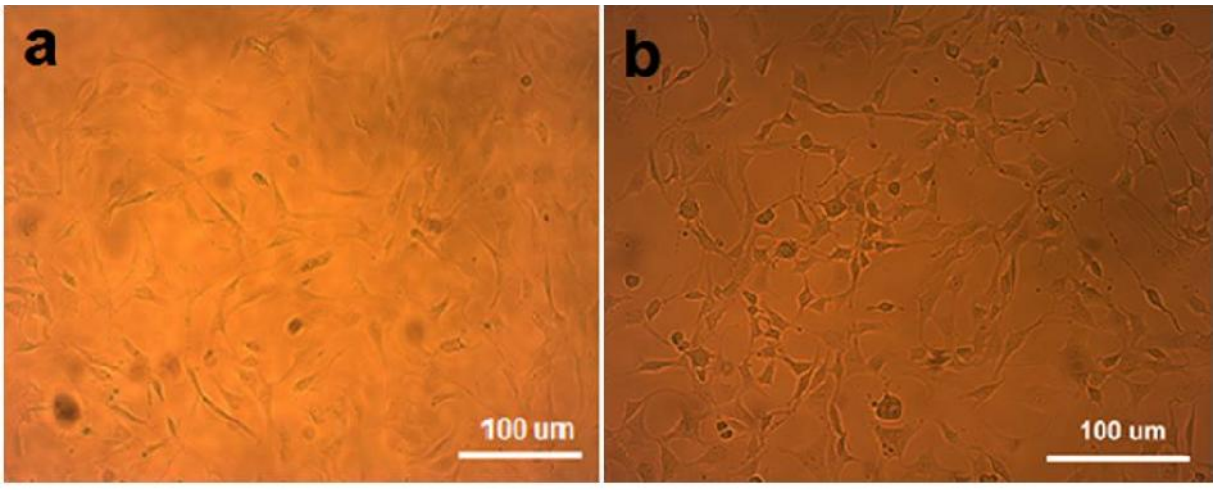


**Fig. 1. Morphology of fibroblastic cells.** a: before inactivation; b: after inactivation by mitomycin C.





[ DOI: 10.22088/IJMCM.BUMS.8.1.24 ]

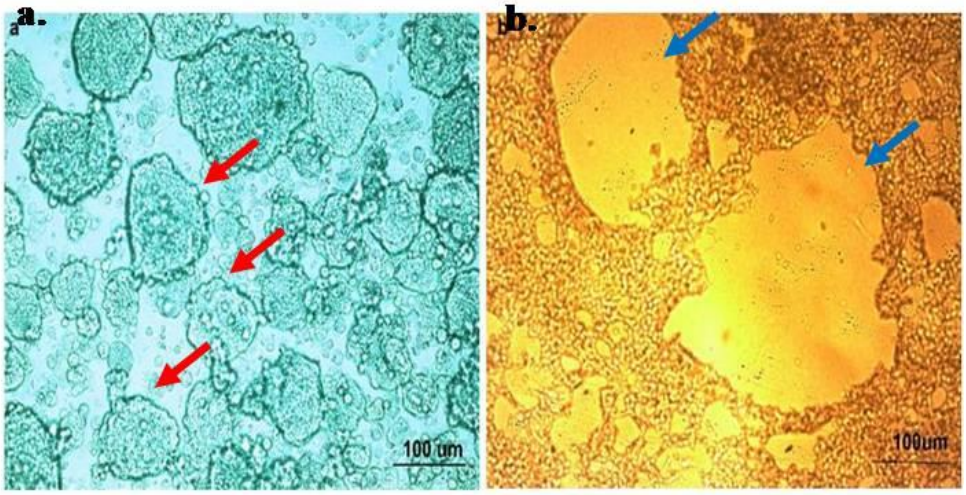


**Fig. 2. Light microscope image of embryoid bodies (EB) formation. a:** hiPSCs EB cells; b: empty spaces after separation of hiPSCs colonies. Red arrows show EB cells, and the cell free position is marked with blue arrows..

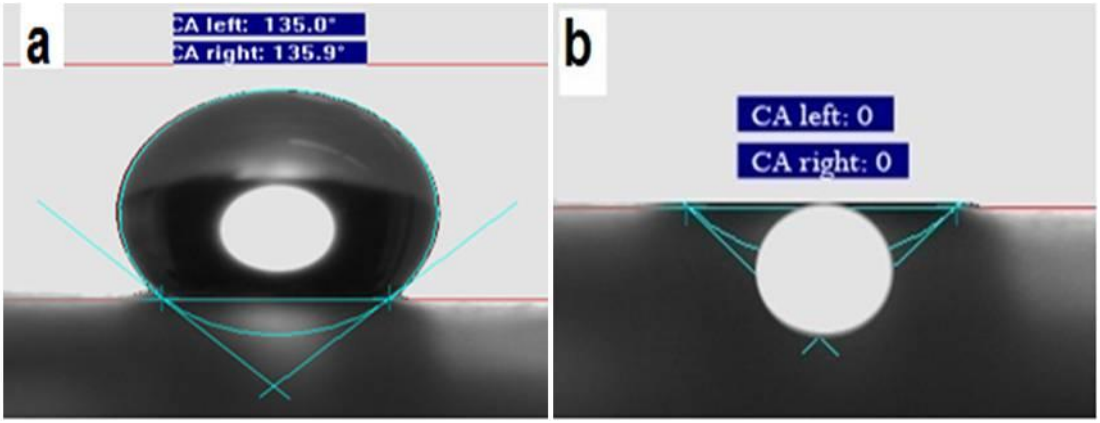


**Fig. 3. The hydrophilicity of nanoscaffold. a: non-plasma PANi-GEL-PCL; b: plasma treatment of PANi-GEL-PCL with NH3.**

**Embryoid bodies (EB) formation**

The hiPSCs colonies turn into embryonic or tubular structures after sufficient growth to begin differentiation. The proper formation of these spherical structures plays an important role in the differentiation of cells into different classes. For this purpose, colonies of hiPSCs were isolated as a layer of isolated nutritional cells (Fig. 2a) by collagenase IV and transferred to the non- adhesive six-well plates containing EB medium. The spherical shapes of EB were visible after 3 days (Fig. 2b).

**Plasma treatment and contact angle measurement of modified nanoscaffolds**

To study the effect of plasma on the hydrophilicity of nanofibers' surfaces, a sample of non-plasma PANi-GEL-PCL nanoscaffold and a plasma PANi-GEL-PCL sample were examined to compare the contact angle (Fig. 3). Fig. 3a represented an angle of 135° that after plasma treatment the angle was reduced to zero (Fig. 3b). This test shows that the presence of $NH_2$ functional groups caused by ammonia gas plasma hydrophilized significantly the surfaces of nano-scaffolds.

**Morphology and size distribution of nanoscaffolds and nanoparticles using SEM**

The PANi-GEL-PCL scaffolds had a comp-





[ DOI: 10.22088/IJMCM.BUMS.8.1.24 ]

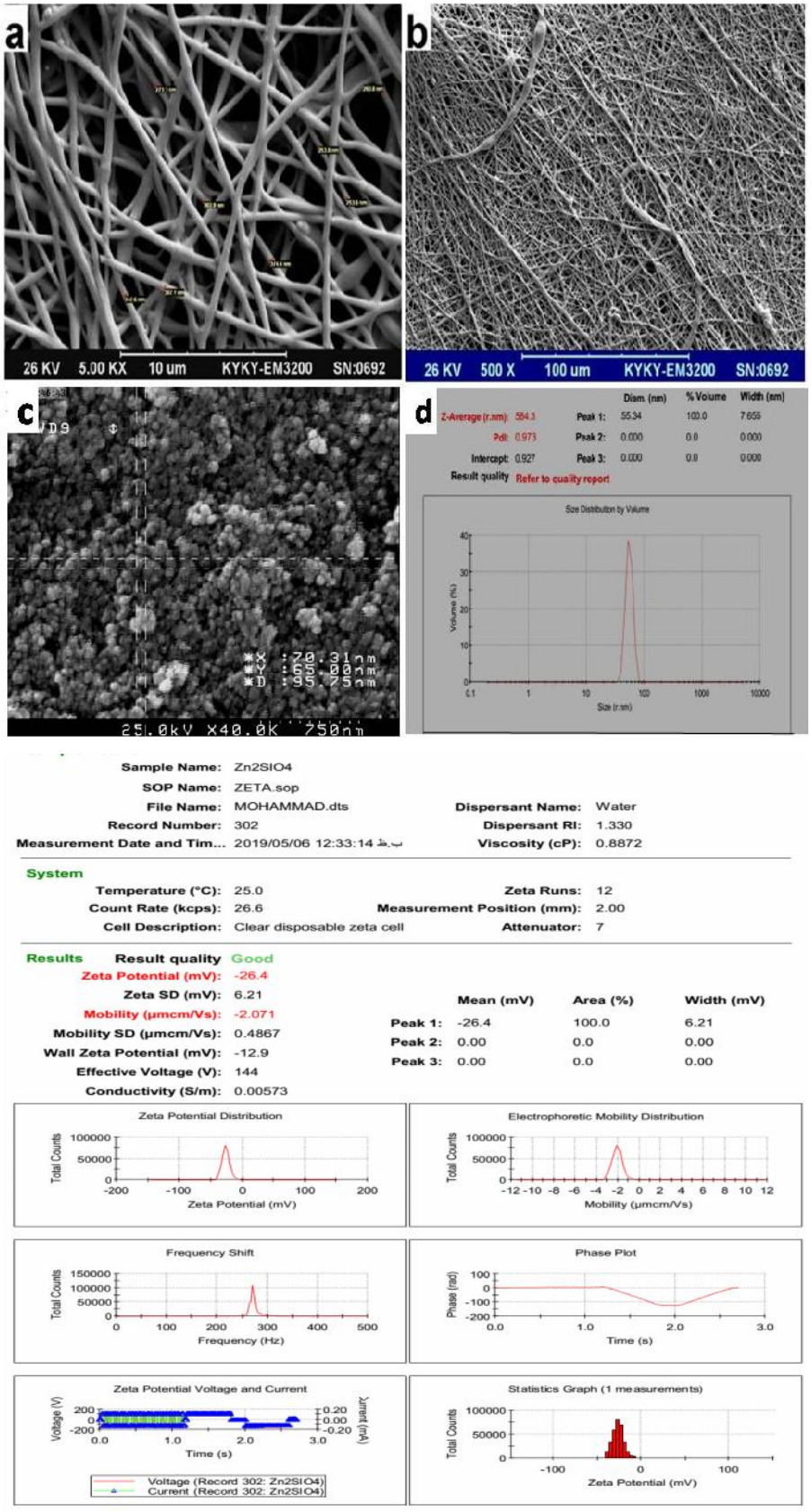


**Fig. 4. Scanning electron microscopy analysis of PANi-GEL-PCL scaffolds.** a: nanofibers without nanoparticles; b: nanofibers with willemite bio-ceramic nanoparticles; c: shape and size distribution of willemite nanoparticles; d: dynamic light scattering (DLS) analysis of willemite nanoparticles; e: zeta potential of Zn2SiO4 nanoparticles was -26.4 mV.





[ DOI: 10.22088/IJMCM.BUMS.8.1.24 ]

letely porous and defect-free structure, and the shape of the fibers was quite uniform (Fig. 4a, b). The fiber diameter was measured between 258-387 nm. After surface modifications and coating with willemite nanoparticles, it became clear that these surface changes had no effects on the diameter and shape of the fibers. Bioceramic nanoparticles bonded to nanoscaffolds through electrostatic forces and shape of these nanoparticles were shown in Fig. 4c.

**Dynamic light scattering measurements for willemite nanoparticles**

Dynamic light scattering indicated a narrow hydrodynamic diameter profile of nanoparticles between 35 to 90 nm, which has a sharp peak around 55 nm with Z-average = 584.3 nm and poly dispersity index (PDI) = 0.973 (Fig. 4d). Zeta potential of Zn2SiO4 nanoparticles was -26.4 mV (Fig. 4e).

**Survival analysis by MTT assay**

The biocompatibility of scaffolds was determined through testing the mitochondrial metabolic activity by MTT method, which indicates the growth and proliferation of cells on the culture plate. As shown in Figure 5, there were significant differences between the fibrous and control groups on the first and fourth days, which reached the lowest level on the seventh day. It is worth noting that the groups containing fiber and nanoparticles yielded the best results throughout the days.

**Alizarin Red staining**

After 14 days of cell differentiation into osteoblasts, the cells cultured on the plate were stained with Alizarin Red to confirm bone differentiation (Fig. 6a). The results showed that the highest calcium deposition occurred in fibers containing nanoparticles. Fibers without nanoparticles also had a better calcium deposit than the group with nanoparticles alone. And the control group had the lowest calcium deposition rate.

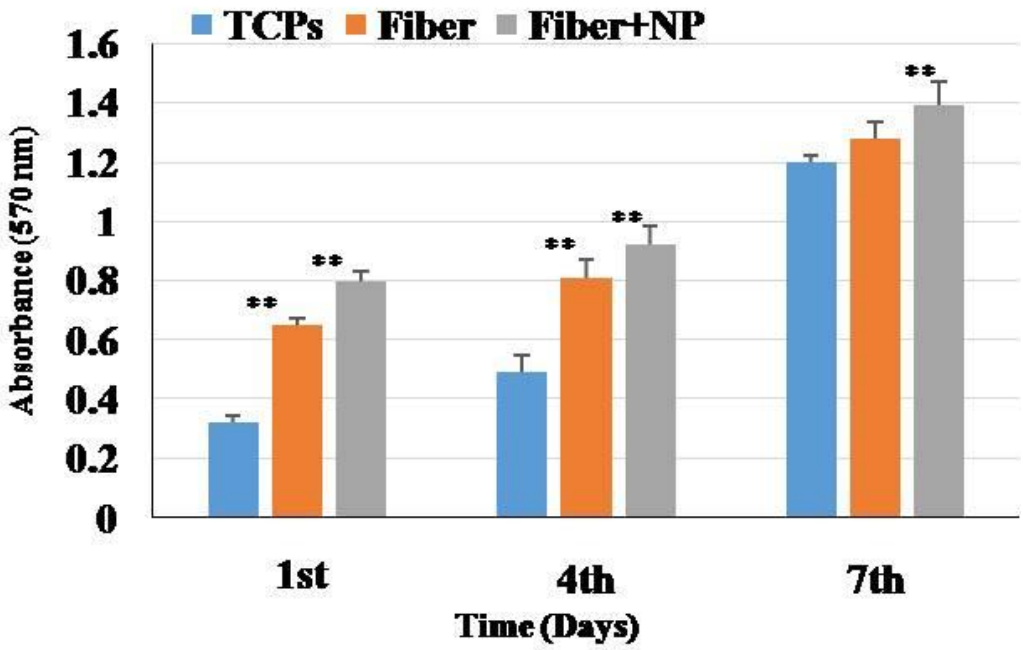


**Fig. 5. MTT analysis of cultured hiPSCs cells.** TCPs: test control groups; Fibers: fibers without nanoparticles; Fiber+NP: nanofibers containing willemite nanoparticles. Asterisk indicates significant difference between the groups at **P < 0.01.





[ DOI: 10.22088/IJMCM.BUMS.8.1.24 ]

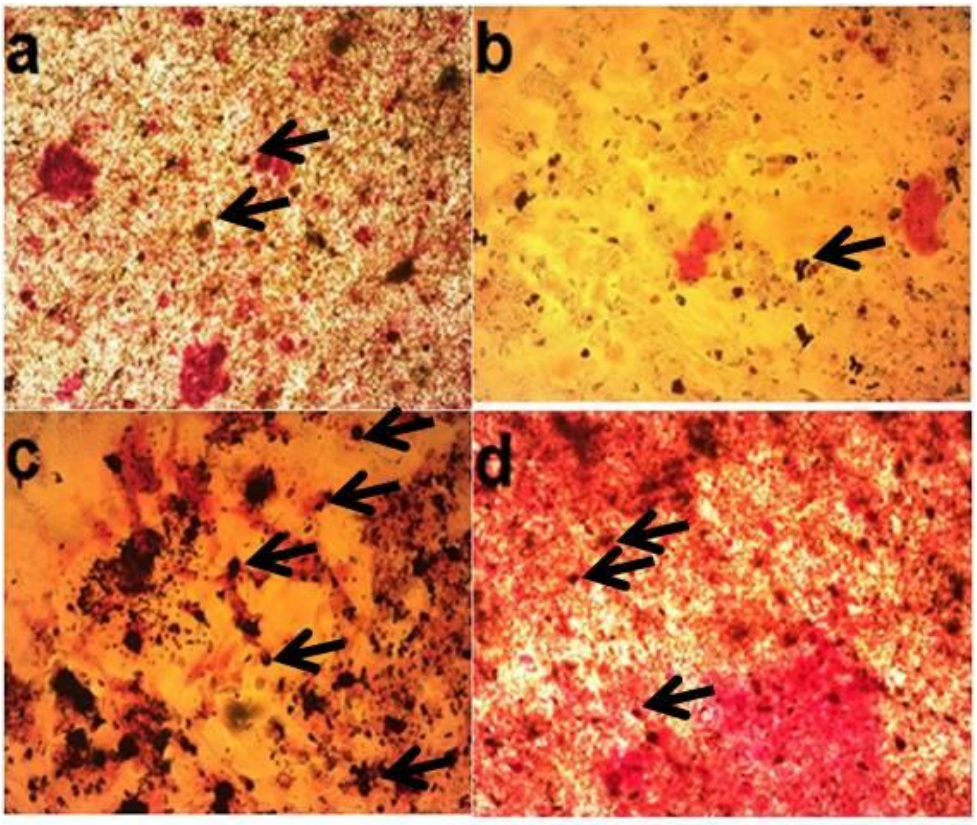


**Fig. 6. Morphology of bone colonies.** a: TCPs (test control groups; b: fibers (fibers without nanoparticles); c: nanofibers containing llemite nanoparticles; d: nanoparticles. The results showed that the highest calcium deposition occurred in fibers containing nanoparticles. The calcium deposition was shown with black arrows. Fibers without nanoparticles also had a better calcium deposit in comparison with nanoparticles (alone) group.

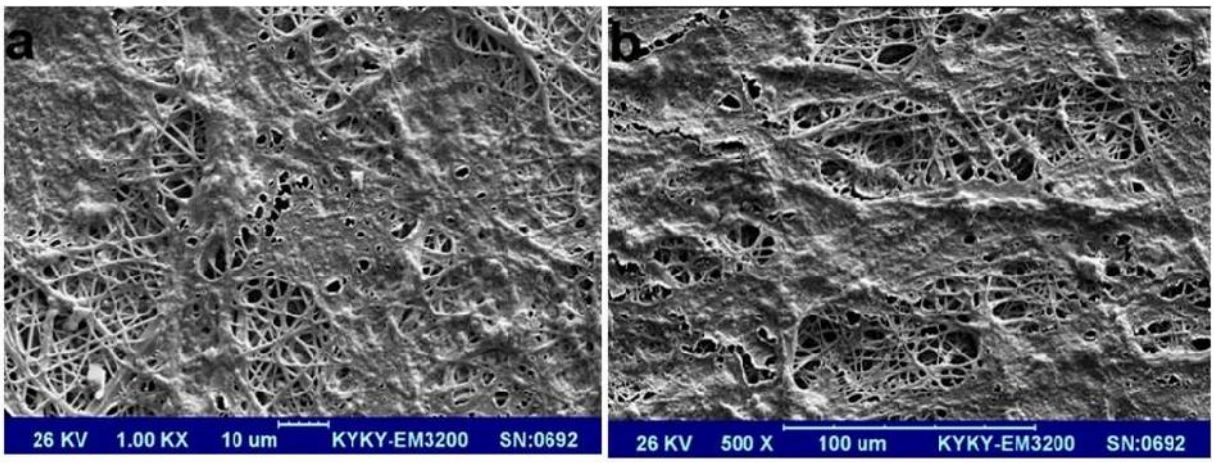


**Fig. 7. Morphology of differentiated hiPSCs into osteoblasts.** a: nanoparticle-contained nanofibers; b: nanoparticle-free nanofibers. Cells cultured on scaffolds coated with nanoparticles were better differentiated in comparison with nanoparticle-free nanofibers. In both groups (a and b) cells were attached and proliferated.

**Cell morphology evaluation after differentiation**

The morphology of cells differentiated after 14 days was examined by electron microscopy (for the cells cultured on scaffolds coated with nanoparticles and those without nanoparticles, Figure 7a shows the morphology of differentiated hiPSCs into osteoblasts on nanoparticle-contained nano-fibers, and figure 7 b represents osteoblasts differentiated hiPSCs nanoparticle-free nano-fibers.

**Alkaline phosphatase activity and mineral deposits**

Although alkaline phosphatase activity was





[ DOI: 10.22088/IJMCM.BUMS.8.1.24 ]

used to assess the osteogenic differentiation of hiPSCs on control group (TCPs), nanofibers without and with nanoparticles as well as willemite nanoparticles on days 7 and 14 (Fig. 8). Alkaline phosphatase enzyme expression in nanofibers containing nanoparticles was higher than other groups on day 7 ($P \leq 0.05$). In addition, remarkably higher levels of alkaline phosphatase expression and activity were seen on nanofibers containing nanoparticles after a 14- day culture under osteogenic differentiation medium.

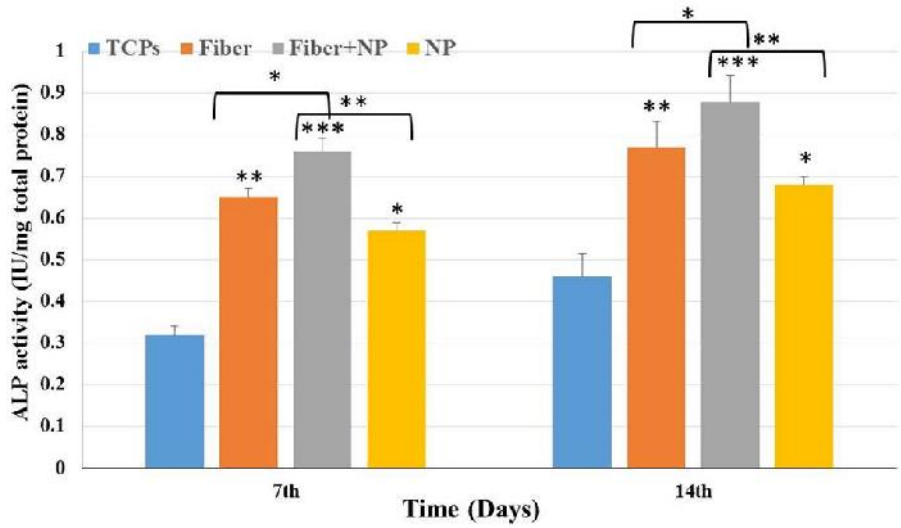


**Fig 8. Alkaline phosphatase activity in cultured hiPSCs.** The GEL-PCL-PANi scaffold containing nanoparticles showed the highest alkaline phosphatase activity during bone differentiation. The nanoparticle-free scaffold played more activity than samples with nanoparticles only. TCPs: test control groups; Fibers: fibers without nanoparticles; Fiber+NP: nanofibers containing willemite nanoparticles; NP: willemite nanoparticles. Asterisks indicate significant difference between the groups at *P < 0.05, **P < 0.01, ***P < 0.001.

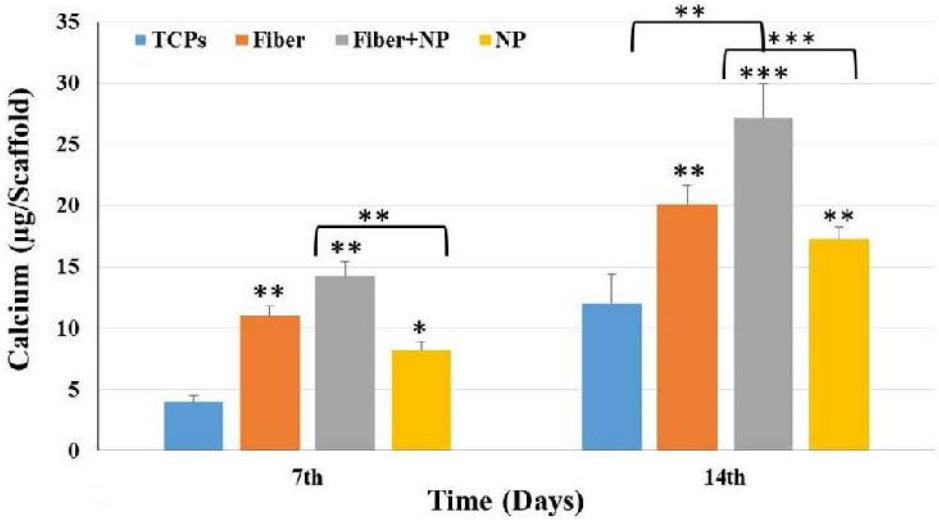


**Fig 9.** The amount of calcic mineral salts deposited on hiPSCs cultured on scaffolds during bone differentiation. TCPs: test control groups; Fibers: fibers without nanoparticles; Fiber+NP: nanofibers containing willemite nanoparticles; NP: willemite nanoparticles. Asterisks indicate significant difference between the groups at *P < 0.05, **P < 0.01, ***P < 0.001.





[ DOI: 10.22088/IJMCM.BUMS.8.1.24 ]

Calcium deposition was also evaluated as the final marker for differentiation into osteoblasts (Fig. 9). Significant increases in calcium deposition were observed in the samples containing scaffolds and nanoparticles compared to the control group on the seventh and 14$^{th}$ day. The results showed that nanoparticle-free fibers, nanoparticles alone, and control group were placed in the next positions, respectively.

## Discussion

Tissue engineering focuses on the development of biological replacements for the restoration, maintenance, and improvement of tissue and organ functions (18). The presence of hydrophilicity in the extracellular matrix facilitates the transfer of gases, nutrients, and excretions at all cellular levels. Furthermore, the presence of nanotopography has a considerable effect on the induction of pathways involved in signaling for the phenotype formation and the fate of cell (18, 19). Recent conductive polymers have received a great attention in the field of biological work such as tissue engineering (15). Many studies have been conducted based on the assumption that many cellular processes, such as adhesion, growth, transfer, and differentiation can be affected by electrical stimulation. Among the conductive polymers, polyaniline has attracted much attention in tissue engineering, the biocompatibility of which has been suggested in previous studies. Most investigations, however, examined the film structures of polyaniline (13).

Gelatin as a natural polymer can be combined with other polymers and provide highly favorable nanoparticles by using a suitable solvent (10). Compared to other biodegradable polymers, PCL has a slow degradation process. This unique feature can provide a biodegradable polymer suitable and sustainable medium for cell culture. Although most of the materials used in tissue engineering are used in their pure forms (i.e. only a single compound is used), a single polymer usually does not meet all the requirements for application in tissue engineering.

Yamanaka and Takahashi (2006) changed the genetic program of murine embryonic fibroblasts through ectopic expression of only four transcription factors and attained a new type of pluripotent stem cells called hiPSCs (20, 21), which can be used to produce disease analysis patterns, drug production, and transplantation science. Biologically active substances can stimulate bodily response, which can be classified into osteogenesis inducers and osteogenerators in bone tissue engineering. Bone-regeneration materials (e.g. synthetic hydroxyapatite ceramics) bind to the bone and stimulate growth at the bone fringes, while bone inducers (e.g. bioactive glasses) motivate the growth of new bone within the materials (21, 22). According to previous investigations on the induction of osteogenesis, this study also used willemite bio-ceramic nanoparticles (Zn2Si4) to enhance the differentiation of hiPSCs into osteoblasts through the supply of Zn minerals required for osteogenesis (23). This research is the first to concurrently investigate bone differentiation via a composite scaffold with PANi-GEL-PCL composition along with willemite bio-ceramic nanoparticles. It was assumed that a series of nano-fibrous stem cells under a bone differentiation environment would lead to the production of a high-potential scaffold to be used in bone tissue engineering. In other words, both types of scaffolds (with/without nanoparticles) showed to be capable of creating a suitable substrate for cell adhesion and growth. However, this ability was observed to be higher in nanofibers containing bio-ceramic nanoparticles than those without nanoparticles. The increased growth rate of cells cultured on nanofibers containing nanoparticles compared to those without nanoparticle could have arisen from the increased bone induction owing to the presence of required minerals, the synergistic effect of which





[ DOI: 10.22088/IJMCM.BUMS.8.1.24 ]

in boosting the adhesion and growth of cells on the surfaces of biomaterials have been studied in detail (24, 25).

Alkaline phosphatase is an enzyme playing a key role in the mineralization of osseous matrix by digesting the phosphate group of phosphate substrates, which usually occurs before the precipitation onset of calcium salts (26). Thus, elevated activity of this enzyme is considered as an early indicator of ossified stem cells, which has previously been reported in hiPSCs (27) and unlimited bodily cells (28). A similar trend of enzyme activity was observed on the scaffolds and flasks in this study. The higher activity of this enzyme on PANi-GEL-PCL nanofibers containing willemite bio-ceramic nanoparticles compared to the other surfaces indicates a willemite boosting effect on the early stages of bone differentiation in hiPSCs.

In addition to alkaline phosphatase activity, calcic sediments account for a major criterion for the production of bone-like cells from stem cells (29, 30). Calcic minerals are naturally produced in a fully organized process, during which the cells cause the peripheral calcium ions to deposit on PANi-GEL-PCL nanofibers (31). The effect of coating nanofibers with nanoparticles in accelerating the process of bone differentiation of stem cells was further confirmed by the higher calcic deposits on nanoparticle-contained nanofibers. It is noteworthy that the difference between precipitation of mineral salts and alkaline phosphatase activity on the nanofibers compared to the flask surface indicates a positive effect of the structure on bone differentiation of stem cells. The unique structure of mineral deposits formed on nanoparticle-borne nanofibers can ideally simulate the inorganic phase of normal osseous tissue.

The present study showed that the formation of a bio-ceramic alongside biocompatible nanofibers and osteoblasts produced from hiPSCs can provide a suitable complex to be used in bone tissue engineering.

In another study, Mengyan Li et al. (2005) examined the properties of PANi-GEL nanoscaffolds and their effects on cell growth and proliferation (32). They concluded that such scaffolds support cellular growth and differentiation. In the present study, more suitable properties have been added to the composite for tissue engineering by inclusion of PCL, which provides a suitable medium for tissue engineering because of its slow degradability.

Finally, it can be stated that each individual group used in this study can support the differentiation of stem cells into osteoblasts. In similar studies, one or two combined polymers have been used in such a design for differentiation. Our study is the first to apply a composite nanoscaffold with PANi-GEL-PCL composition for differentiation of hiPSCs. The results signify that the nanoscaffolds used together with bio-ceramic nanoparticles could well support the differentiation. This could have resulted from the combined special properties of polyaniline for electrical conductivity along with gelatin biocompatibility and timed PCL degradability.

In conclusion, the results obtained in this study clearly demonstrated the high efficiency of electrospinned composite scaffolds. As with similar studies, willemite bio-ceramic nanoparticles showed to be efficient in the acceleration and improvement of differentiation. It is worth noting that here the electrospinned scaffolds not only helped differentiate stem cells, but also improved cell growth, which might be owing to the unique combination of these three polymers in a homologous matrix. Despite the fact that application of this fiber in tissue engineering is long-reaching, the properties of this composite along with willemite nanoparticles can be a good context to tissue engineering tasks.

**Acknowledgment**

We are grateful to the manager of Stem Cell





[ DOI: 10.22088/IJMCM.BUMS.8.1.24 ]

Technology Research Center (Tehran, Iran) and Baqiyatallah University of Medical Sciences (Tehran, Iran).

**Conflict of interest**

The authors declare that they have no conflict of interest.

## References

1. Amani HME, Arzaghi H, Davaran S. Three-Dimensional Graphene Foams: Synthesis, Properties, Biocompatibility, Biodegradability, and Applications in Tissue Engineering. ACS Biomater Sci Eng 2019;5:193-214.

2. Griffith LG. Emerging design principles in biomaterials and scaffolds for tissue engineering. Ann N Y Acad Sci 2002;961:83-95.

3. Ji W, Sun Y, Yang F, et al. Bioactive electrospun scaffolds delivering growth factors and genes for tissue engineering applications. Pharm Res 2011;28:1259-72.

4. Chaput C, Selmani A, Rivard CH. Artificial scaffolding materials for tissue extracellular matrix repair. Curr Opin Orthop 1996;7:62-8.

5. Venugopal JR, Zhang Y, Ramakrishna S. In vitro culture of human dermal fibroblasts on electrospun polycaprolactone collagen nanofibrous membrane. Artif Organs 2006;30:440-6.

6. He W, Ma Z, Yong T, et al. Fabrication of collagen-coated biodegradable polymer nanofiber mesh and its potential for endothelial cells growth. Biomaterials 2005;26:7606-15.

7. Smith LA, Ma PX. Nano-fibrous scaffolds for tissue engineering. Colloids Surf B Biointerfaces 2004;39:125-31.

8. Kim BS, Mooney DJ. Development of biocompatible synthetic extracellular matrices for tissue engineering. Trends Biotechnol 1998;16:224-30.

9. Li M, Mondrinos MJ, Chen X, et al. Co-electrospun poly(lactide-co-glycolide), gelatin, and elastin blends for tissue engineering scaffolds. J Biomed Mater Res A 2006;79:963-73.

10. Zhong SP, Teo WE, Zhu X. Development of a novel collagen–GAG nanofibrous scaffold via electrospinning. Mater Sci Eng C 2007;27:262-6.

11. Kooshki H, Ghollasi M, Halabian R, et al. Osteogenic differentiation of preconditioned bone marrow mesenchymal stem cells with lipopolysaccharide on modified poly-l-lactic-acid nanofibers. J Cell Physiol 2019;234:5343-53.

12. Bidez PR, 3rd, Li S, Macdiarmid AG, et al. Polyaniline, an electroactive polymer, supports adhesion and proliferation of cardiac myoblasts. J Biomater Sci Polym Ed 2006;17:199-212.

13. Bryan AH. Trace elements in human and animal nutrition. Am J Public Health Nations Health 1957;47:496.

14. Weissman IL. Stem cells: units of development, units of regeneration, and units in evolution. Cell 2000;100:157-68.

15. Madonna R. Human-induced pluripotent stem cells: in quest of clinical applications. Mol Biotechnol 2012;52:193-203.

16. Nelson TJ, Martinez-Fernandez A, Yamada S, et al. Induced pluripotent stem cells: advances to applications. Stem Cells Cloning 2010;3:29-37.

17. Hubbell JA. Biomaterials in tissue engineering. Biotechnology (N Y) 1995;13:565-76.

18. Tan W, Krishnaraj R, Desai TA. Evaluation of nanostructured composite collagen--chitosan matrices for tissue engineering. Tissue Eng 2001;7:203-10.

19. Takahashi K, Yamanaka S. Induction of pluripotent stem cells from mouse embryonic and adult fibroblast cultures by defined factors. Cell 2006;126:663-76.

20. Rose FR, Oreffo RO. Bone tissue engineering: hope vs hype. Biochem Biophys Res Commun 2002;292:1-7.

21. Wright V, Peng H, Usas A, et al. BMP4-expressing muscle-derived stem cells differentiate into osteogenic lineage and improve bone healing in immunocompetent mice. Mol Ther 2002;6:169-78.

22. Ishikawa K, Miyamoto Y, Yuasa T, et al. Fabrication of Zn containing apatite cement and its initial evaluation using human osteoblastic cells. Biomaterials 2002;23:423-8.

23. Kim CH, Khil MS, Kim HY, et al. An improved hydrophilicity via electrospinning for enhanced cell attachment and proliferation. J Biomed Mater Res B Appl Biomater 2006;78:283-90.

24. Yang J, Bei J, Wang S. Improving cell affinity of poly (D, L lactide) film modified by anhydrous ammonia plasma treatment. Polym Adv Technol 2002;13:220-26.

25. Anderson HC, Sipe JB, Hessle L, et al. Impaired calcification around matrix vesicles of growth plate and bone in alkaline phosphatase-deficient mice. Am J Pathol 2004;164:841-7.

26. Jaiswal N, Haynesworth SE, Caplan AI, et al. Osteogenic differentiation of purified, culture-expanded human mesenchymal stem cells in vitro. J Cell Biochem 1997;64:295-





[ DOI: 10.22088/IJMCM.BUMS.8.1.24 ]

312.

27. Kogler G, Sensken S, Airey JA, et al. A new human somatic stem cell from placental cord blood with intrinsic pluripotent differentiation potential. J Exp Med 2004;200:123-35.

28. Halvorsen YD, Franklin D, Bond AL, et al. Extracellular matrix mineralization and osteoblast gene expression by human adipose tissue-derived stromal cells. Tissue Eng 2001;7:729-41.

29. zur Nieden NI, Kempka G, Ahr HJ. In vitro differentiation of embryonic stem cells into mineralized osteoblasts. Differentiation 2003;71:18-27.

30. Li M, Mondrinos MJ, Chen X, et al. Electrospun blends of natural and synthetic polymers as scaffolds for tissue engineering. Conf Proc IEEE Eng Med Biol Soc 2005;6:5858-61.



[ DOI: 10.22088/IJMCM.BUMS.8.1.24 ]